



Defense Threat Reduction Agency
8725 John J. Kingman Road, MS 6201
Fort Belvoir, VA 22060-6201



DTRA-TR-03-17

TECHNICAL REPORT

Laser Wavefront Analyzer for Gas Puff Loads on Decade Quad

Approved for public release; distribution is unlimited.

April 2006

20060508026

DTRA 01-99-D-0043

N. Qi, et al.

Prepared by:
Alameda Applied Sciences
Corporation
626 Whitney Street
San Leandro, CA 94577

DESTRUCTION NOTICE

FOR CLASSIFIED documents, follow the procedures in DoD 5550.22-M, National Industrial Security Program Operating Manual, Chapter 5, Section 7 (NISPOM) or DoD 5200.1-R, Information Security Program Regulation, Chapter 1X.

FOR UNCLASSIFIED limited documents, destroyed by any method that will prevent disclosure of contents or reconstruction of the document.

Retention of this document by DoD contractors is authorized in accordance with DoD 5220.22M, Industrial Security manual.

PLEASE NOTIFY THE DEFENSE THREAT REDUCTION AGENCY, ATTN: IMMI, 8725 JOHN J. KINGMAN ROAD, MS-6201, FT. BELVOIR, VA 22060-6201. IF YOUR ADDRESS IS INCORRECT, IF YOU WISH IT DELETED FROM THE DISTRIBUTION LIST, OR IF THE ADDRESSEE IS NO LONGER EMPLOYED BY YOUR ORGANIZATION.

DISTRIBUTION LIST UPDATE

This mailer is provided to enable DTRA to maintain current distribution lists for reports. (We would appreciate you providing the requested information.)

- ☐ Add the individual listed to your distribution list.
- ☐ Delete the cited organization/individual.
- ☐ Change of address.

Note:

Please return the mailing label from the document so that any additions, changes, corrections or deletions can be made easily. For distribution cancellation or more information call DTRA/BDMI (703) 767-4724.

NAME: _____

ORGANIZATION: _____

OLD ADDRESS

NEW ADDRESS

TELEPHONE NUMBER: () _____

DTRA PUBLICATION NUMBER/TITLE

CHANGES/DELETIONS/ADDITONS, etc.

(Attach Sheet if more Space is Required)

DTRA or other GOVERNMENT CONTRACT NUMBER: _____

CERTIFICATION of NEED-TO-KNOW BY GOVERNMENT SPONSOR (if other than DTRA):

SPONSORING ORGANIZATION: _____

CONTRACTING OFFICER or REPRESENTATIVE: _____

SIGNATURE: _____

REPORT DOCUMENTATION PAGE			Form Approved OMB No. 0704-0188	
Public reporting burden for this collection of information is estimated to average 1 hour per response, including the time for reviewing instructions, searching existing data sources, gathering and maintaining the data needed, and completing and reviewing the collection of information. Send comments regarding this burden, estimate or any other aspect of this collection of information, including suggestions for reducing this burden, to Washington Headquarters Services, Directorate for Information Operations and Reports, 1215 Jefferson Davis Highway, Suite 1204, Arlington, VA 22202-4302, and to the Office of Management and Budget, Paperwork Reduction Project (0704-0188), Washington, DC 20503.				
1. AGENCY USE ONLY (Leave blank)		2. REPORT DATE April 2006		3. REPORT TYPE AND DATES COVERED
4. TITLE AND SUBTITLE Laser Wavefront Analyzer for Gas Puff Loads on Decade Quad		5. FUNDING NUMBERS C - DTRA 01-99-D-0043 PE - 131D PR - OH TA - OO WU - DH00669		
6. AUTHOR(S) N. Qi, K. Campbell, A. Bixler, R. Prasad, P. Coleman and M. Krishnan		8. PERFORMING ORGANIZATION REPORT Aasc02TM-06		
7. PERFORMING ORGANIZATION NAME(S) AND ADDRESS(ES) Alameda Applied Sciences Corporation 626 Whitney Street San Leandro, CA 94577		10. SPONSORING/MONITORING AGENCY REPORT NUMBER DTRA-TR-03-17		
9. SPONSORING/MONITORING AGENCY NAME(S) AND ADDRESS(ES) Defense Threat Reduction Agency 8725 John J. Kingman Road, MSC 6201 Fort Belvoir, VA 22060-6201 NTES/R. DAVIS		11. SUPPLEMENTARY NOTES This work was sponsored by the Defense Threat Reduction Agency under RDT&E RMC codeB 131D D 4000 OH OO 00669 25904D		
12a. DISTRIBUTION/AVAILABILITY STATEMENT Approved for public release; distribution in unlimited.		12b. DISTRIBUTION CODE		
13. ABSTRACT (Maximum 200 words) The Objective of this contract was to develop and implement a Laser Wavefront Analyzer (LWA) to measure z-pinch initial gas density profiles suitable for the Decade Quad Simulator (DQ) at AEDC, TN. A probe laser beam passes through a supersonic gas jet, which distorts the laser wavefronts. The LWA measures such wavefront distortions which are in the range of $\sim \lambda/50$. We have designed, constructed and validated our prototype LWA. Gas densities, produced by using DQ gas puff hardware, have been measured. This report summarizes our results. The advantage of the LWA is that the gas density profile can be obtained within one or few shots. However, in the present LWA configuration, the air density-length product ($\sim 10^{21} \text{ cm}^{-2}$) along the line of sight is much higher than that of gas puff ($\sim 10^{18} \text{ cm}^{-2}$). Variations in the air column limit the present arrangement to a sensitivity of $: 5 \times 10^{17} \text{ cm}^{-3}$. We have observed in related Fiber Optic Interferometer (FOI) measurements that the time scale of the air turbulence is on the order of 1 ms. The effects of the air turbulence can be minimized to a factor of ≈ 10 when the reference image is taken within $\approx 500 \mu\text{s}$ of the gas measurement image by using two laser probe beams and/or by putting the LWA in a vacuum to reduce the air density-length product. With these improvements, the position uncertainty of the microlens focal spots can be reduced from the present 0.1 pixel to 0.01 pixels.				
14. SUBJECT TERMS Microlens Torp Refraction		15. NUMBER OF PAGES 20		
17. SECURITY CLASSIFICATION OF THIS PAGE UNCLASSIFIED		18. SECURITY CLASSIFICATION OF REPORT UNCLASSIFIED		19. SECURITY CLASSIFICATION OF ABSTRACT UNCLASSIFIED
				20. LIMITATION OF ABSTRACT SAR

CONVERSION TABLE

Conversion Factors for U.S. Customary to metric (SI) units of measurement.

MULTIPLY \longrightarrow BY \longrightarrow TO GET
 TO GET \longleftarrow BY \longleftarrow DIVIDE

angstrom	1.000 000 x E -10	meters (m)
atmosphere (normal)	1.013 25 x E +2	kilo pascal (kPa)
bar	1.000 000 x E +2	kilo pascal (kPa)
barn	1.000 000 x E -28	meter ² (m ²)
British thermal unit (thermochemical)	1.054 350 x E +3	joule (J)
calorie (thermochemical)	4.184 000	joule (J)
cal (thermochemical/cm ²)	4.184 000 x E -2	mega joule/m ² (MJ/m ²)
curie	3.700 000 x E +1	*giga bacquerel (GBq)
degree (angle)	1.745 329 x E -2	radian (rad)
degree Fahrenheit	$t_k = (t^{\circ}f + 459.67)/1.8$	degree kelvin (K)
electron volt	1.602 19 x E -19	joule (J)
erg	1.000 000 x E -7	joule (J)
erg/second	1.000 000 x E -7	watt (W)
foot	3.048 000 x E -1	meter (m)
foot-pound-force	1.355 818	joule (J)
gallon (U.S. liquid)	3.785 412 x E -3	meter ³ (m ³)
inch	2.540 000 x E -2	meter (m)
jerk	1.000 000 x E +9	joule (J)
joule/kilogram (J/kg) radiation dose absorbed	1.000 000	Gray (Gy)
kilotons	4.183	terajoules
kip (1000 lbf)	4.448 222 x E +3	newton (N)
kip/inch ² (ksi)	6.894 757 x E +3	kilo pascal (kPa)
ktap	1.000 000 x E +2	newton-second/m ² (N-s/m ²)
micron	1.000 000 x E -6	meter (m)
mil	2.540 000 x E -5	meter (m)
mile (international)	1.609 344 x E +3	meter (m)
ounce	2.834 952 x E -2	kilogram (kg)
pound-force (lbs avoirdupois)	4.448 222	newton (N)
pound-force inch	1.129 848 x E -1	newton-meter (N-m)
pound-force/inch	1.751 268 x E +2	newton/meter (N/m)
pound-force/foot ²	4.788 026 x E -2	kilo pascal (kPa)
pound-force/inch ² (psi)	6.894 757	kilo pascal (kPa)
pound-mass (lbm avoirdupois)	4.535 924 x E -1	kilogram (kg)
pound-mass-foot ² (moment of inertia)	4.214 011 x E -2	kilogram-meter ² (kg-m ²)
pound-mass/foot ³	1.601 846 x E +1	kilogram-meter ³ (kg/m ³)
rad (radiation dose absorbed)	1.000 000 x E -2	**Gray (Gy)
roentgen	2.579 760 x E -4	coulomb/kilogram (C/kg)
shake	1.000 000 x E -8	second (s)
slug	1.459 390 x E +1	kilogram (kg)
torr (mm Hg, 0° C)	1.333 22 x E -1	kilo pascal (kPa)

*The bacquerel (Bq) is the SI unit of radioactivity; 1 Bq = 1 event/s.

**The Gray (GY) is the SI unit of absorbed radiation.

Table of Contents

SECTION	PAGE
CONVERSION TABLE	ii
FIGURES	iv
1. INTRODUCTION.....	1
2. DESIGN FABRICATION AND TEST OF THE LWA.....	5
3. SUMMARY AND CONCLUSIONS.....	10
DISTRIBUTION LIST.....	DL-1

Figures

Figure	Page
1 Schematic of the laser source.....	1
2 Schematic drawing of the LWA detection system	2
3 Probe laser beam passing through the gas puff.....	4
4 The focal spots of the 65x65 microlens array captured by a CCD camera.....	5
5 The difference of the corresponding focal spot positions in two consecutive laser pulses.....	6
6 The differences of the corresponding focal spot positions when the incoming laser wavefront was changes.....	7
7 Schematic drawing of the "recessed" nozzle.....	8
8 Schematic drawing of the "non-recessed" nozzle.....	8
9 FOI measured density as a function of time.....	9
10 Measured gas density.....	10

1 Introduction

Alameda Applied Sciences Corporation was awarded this TORP to develop and implement a Laser Wavefront Analyzer (LWA) to measure z-pinch initial gas density profiles suitable for Decade Quad. A probe laser beam passes through a gas jet, which distorts the laser wavefronts. The instrument (LWA) measures such wavefront distortions which are in the range of $\sim\lambda/50$. We have designed, constructed and validated our prototype LWA. Gas densities, produced by using DQ gas puff hardware, have been measured. This report summarizes our results.

2 Design, fabrication and test of the LWA

The LWA instrumentation consisted of two systems. One is a short pulse, large diameter laser beam and the other is the sensor for laser wavefront analysis. Fig. 1 shows the arrangement of the laser system. The Nd:YAG laser delivers a few mJ, ≈ 5 ns pulse at 532nm wavelength. The laser beam was focused by a 50 cm focal length lens through a ≈ 100 μm diameter pinhole and expanded to ≈ 10 cm in diameter by a combination of negative and positive focal length lenses.

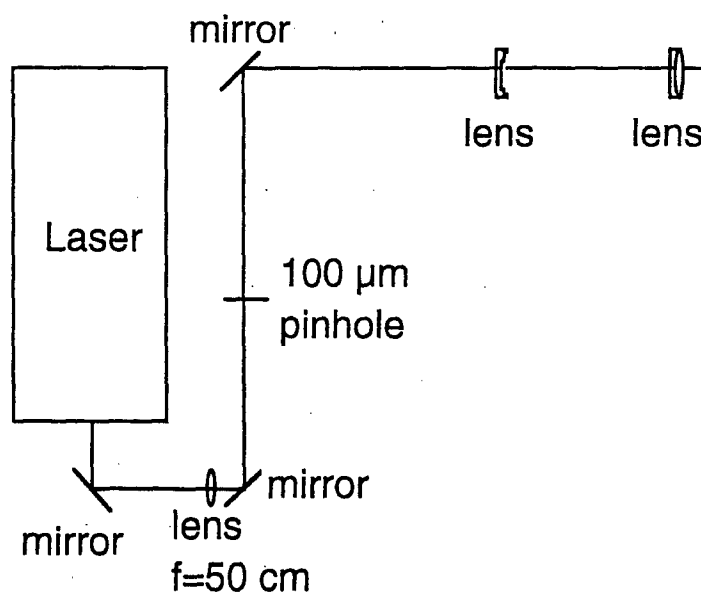


Fig. 1: Schematic of the laser source, which produces a ≈ 5 ns, ≈ 10 cm diameter uniform and collimated beam.

Fig. 2 shows the detection scheme for the laser wavefront. Two lenses image the gas puff on to the microlens array with a demagnification of 3:1. The collimated laser beam passes through the microlens array, which produces an array of bright spots. The focal position of each spot depends on the incident wave surface orientation. The positions of these focal spots are recorded by using a CCD camera. The principles of the LWA follow.

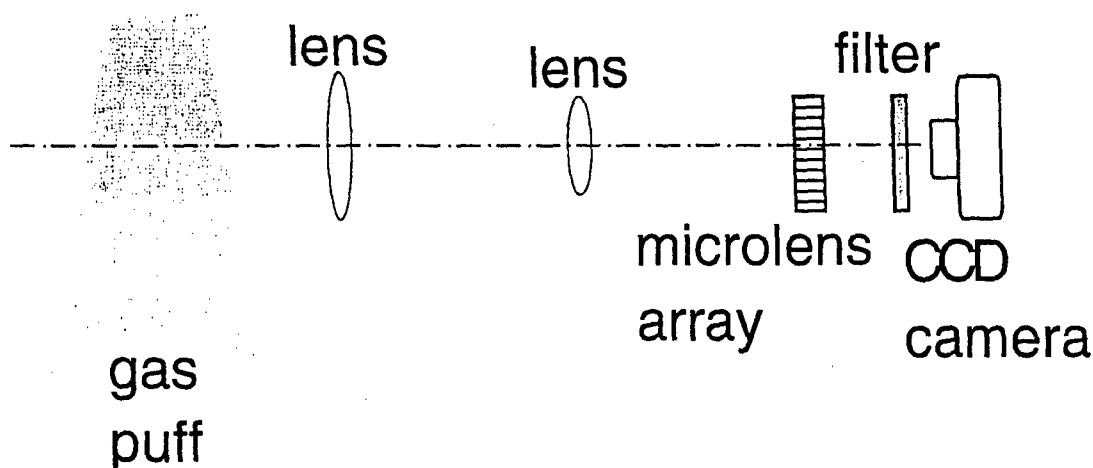


Fig.2: Schematic drawing of the LWA detection system.

When an incident, laser beam traverses the gas (or plasma), it suffers refraction. Refraction by atoms (or electrons) tilts the beam by an angle θ and shifts the phase by Φ . Measurement of θ (or Φ) gives the gas (or electron) density along the chord traversed by the laser. For argon gas, the phase shift Φ and the refractive angular deviation θ of the probe laser beam are described by,

$$\Phi = 6.53 \times 10^{-15} \lambda^{-1} (\text{\AA}) \int n(\text{cm}^{-3}) dl(\text{cm}) \quad \text{rad} \quad (1)$$

and

$$\theta = 1.04 \times 10^{-23} \frac{d}{dx} \int n(\text{cm}^{-3}) dl(\text{cm}) \quad \text{rad} \quad (2)$$

where x is the distance from the axis and λ is the laser wavelength.

Using the Shack-Hartmann method,[1,2] which is a widely used technique for the measurement of wavefront distortions in optical beams and adaptive optics, the phase shifts of the laser beam are derived. Figure 3 shows how the tilt at each sampled point is established, where θ is the angle tilt of the beamlet. Let the wavefront of the distorted probe beam (after passing through the z-pinch plasma) be described as $W(x)$, where x is the coordinate of some

point x in the transverse plane of the un-distorted part of the probe beam. When the displaced wavefront is focused on the test plane, the distorted wavefront $W(x)$ gives the displaced wavefront error at the point $x+\delta x$. The relation between the wavefront distortion $W(x)$ and the x component δx of the ray deviation in the focal plane can be derived with sufficient accuracy using the following approximation:

$$\frac{\partial W}{\partial x} = \frac{\delta x}{d} \quad (3)$$

where d is the separation between the micro lens array and the recording plane. Integrating Eq. 4, we obtain

$$W(x) = \frac{1}{d} \int_0^x \delta x dx \quad (4)$$

If the wavefront deviation W is written in wavelengths by defining $H=W/\lambda$, we have,

$$H(x) = \frac{1}{2d\lambda} \int_0^x \delta x dx \quad (5)$$

Since the function δx is sampled only at discrete points such as the micro-lens array, the integration will be performed by using the trapezoidal rule, yielding

$$H_N = \frac{1}{2d\lambda} \sum_{n=2}^N \frac{\delta x_{n-1} + \delta x_n}{2} \Delta x_{n-1} \quad (6)$$

where Δx_{n-1} is the separation between the points n and $n-1$ (i.e. the micro lens pixels). For constant Δx , we have

$$H_N = \frac{1}{d\lambda} \left(\frac{1}{2} \delta x_1 + \sum_{n=2}^{N-1} \frac{\delta x_{n-1} + \delta x_n}{2} + \frac{1}{2} \delta x_N \right) \Delta x \quad (7)$$

Similarly,

$$H_M = \frac{1}{d\lambda} \left(\frac{1}{2} \delta y_1 + \sum_{n=2}^{M-1} \frac{\delta y_{n-1} + \delta y_n}{2} + \frac{1}{2} \delta y_M \right) \Delta y \quad (8)$$

These expressions give the wavefront deviation at any N th point from some reference point $N=1$. There are also other methods to calculate the wavefront surface with reliable results. In most cases the trapezoidal rule is sufficient.

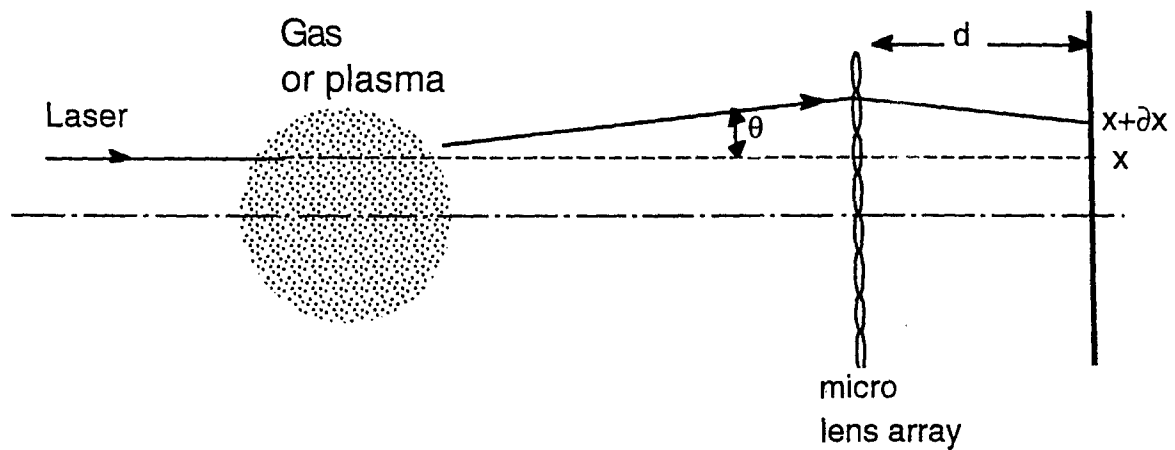


Fig. 3: Probe laser beam passing through the gas puff undergoes changes in its propagation direction due to the atom density gradient.

With the help of Prof. M. Roggemann (our consultant), we selected a 65x65, 0.4 mm lenslet diameter, 54 mm focal length microlens array for the gas puff density measurements. A 2000x3000 pixel monochrome CCD camera was used to detect the position of the microlens focal spots. An example of the resulting image from the CCD camera is shown in Fig. 4.

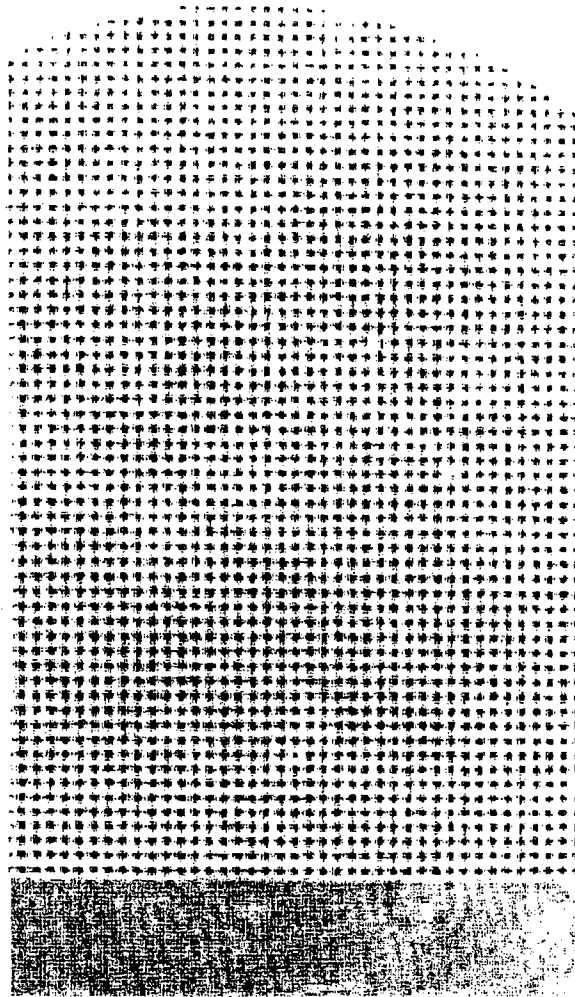


Fig. 4: The focal spots of the 65x65 microlens array captured by a CCD camera. The phase shifts can be derived from the positions of the microlens array focal points.

In the presence of a gas puff, the focal positions of the micro-lenses will change. By taking images with and without the gas puff, these position changes of the focal points can be measured. The change in position is directly proportional to the tilt angle at each sample point. Note per Eq. 1 that the tilt angle is a function of the chordal integral of the density spatial gradient. To derive the density itself, the data must be Abel inverted. Fortunately, that inversion uses the density gradient, hence the raw tilt data do not need to be numerically differentiated and can be directly used in the inversion. Thus, we can derive the laser wavefront surface and the gas density profile. Figure 5 shows the difference of the corresponding focal spot positions in two consecutive laser pulses. The two laser pulses were several seconds apart. There is a constant base line shift of ≈ 0.9 pixels due to the vibration of the vacuum chamber and/or optical tables, where the LWA was mounted. The sample to sample variation, about 0.1 pixels, is a measure of the system noise and thus defines the instrument's sensitivity. Figure 6 shows the differences of

the corresponding focal spot positions when the incoming laser wavefront was changed from a plane wave to a wave with radius of curvature of 18 meters. Data like this establish the calibration factor of the LWA, relating measured focal spot position changes to wavefront tilt.

As shown in Figs. 5 and 6, the typical uncertainty of the position detection is about ± 0.1 pixel. For a 54 mm focal length microlens array and 9 μm pixel size, this gives an angular resolution of $\approx 17 \mu\text{rads}$ or $\frac{d}{dx} \int n(\text{cm}^{-3}) dl(\text{cm}) \approx 1.6 \times 10^{18} \text{cm}^{-3}$. With an optical image system of 3:1 demagnification, the effective sensitivity is $0.3 \times \frac{d}{dx} \int n(\text{cm}^{-3}) dl(\text{cm}) \approx 5 \times 10^{17} \text{cm}^{-3}$. Recalling that air density at one atmosphere is 10^{19}cm^{-3} , the 0.1 pixel “noise” observed here is probably due to minor variations in the 2 meter long air column covered by the laser beam from the source to the detection. That is, our observed sensitivity is limited in these experiments by air density variations (for example, air currents and lab sound noise) in the $2 \times 10^{21} \text{cm}^{-2}$ chordal integral of ambient air.

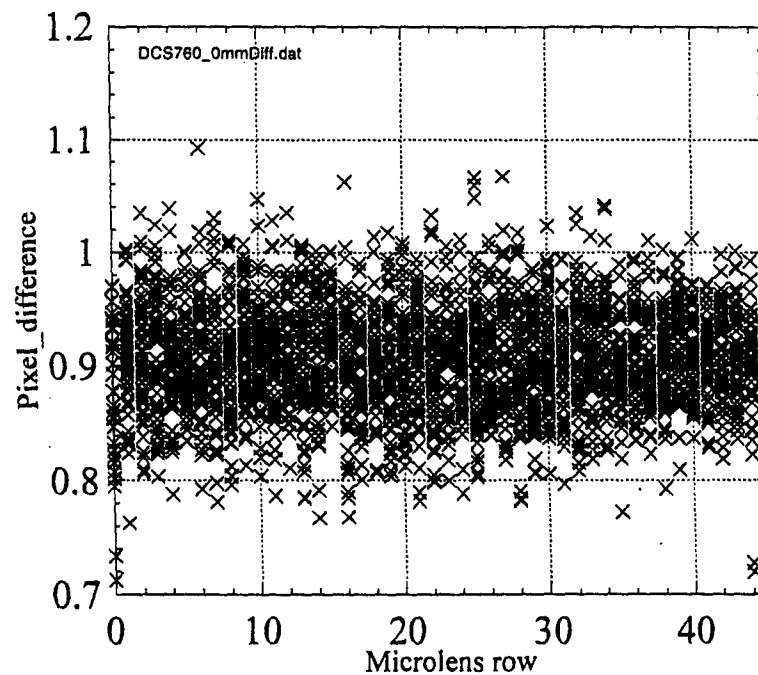


Fig. 5: The difference of the corresponding focal spot positions in two consecutive laser pulses, which was several seconds apart. The ≈ 0.9 pixel base line shift is caused by the vibration of the system and the 0.1 pixel variation is due to the ambient air variation.

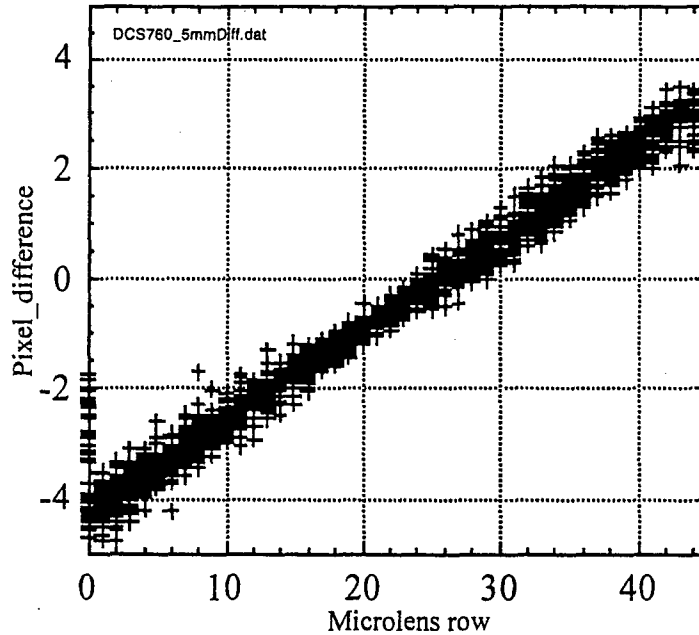


Fig. 6: The differences of the corresponding focal spot positions when the incoming laser wavefront was changed from a plane wave to a wave with radius of curvature of 18 meters.

The laser pulse width, ≈ 5 ns, is short compared to the gas flow time of ≥ 100 μ s. Each LWA image maps the radial and axial gas profile at a particular time during the gas flow. For the experiments reported here, we used “recessed” and “non-recessed” “aerodynamic” nozzles, which have been used in our recent Double-Eagle Argon gas puff experiments. Figs. 7 and 8 are the schematic drawings of these two nozzles. The diameter of the inner throat is 4 cm and the outer 8.7 cm. The difference between these two nozzles is that the “non-recessed” nozzle produces two “distinguished” shell-like gas jets near the nozzle exit, while these two shell gas jets are merged as in the case of the “recessed” nozzle.

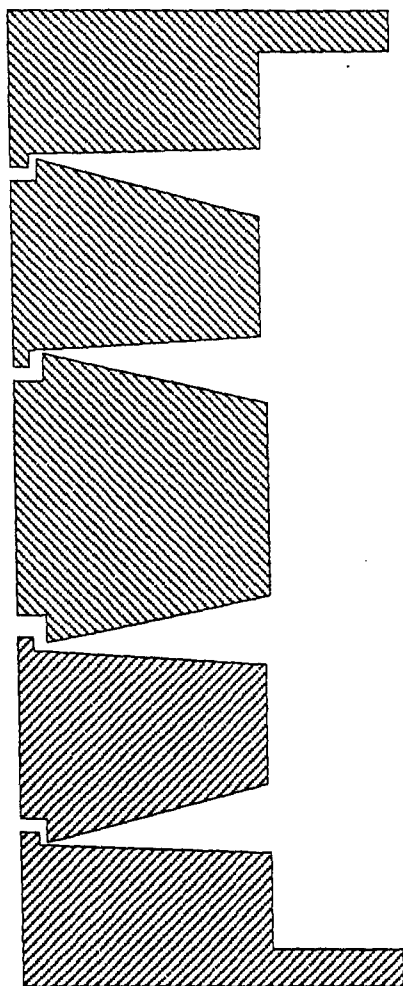


Fig. 7: Schematic drawing of the "recessed" nozzle.

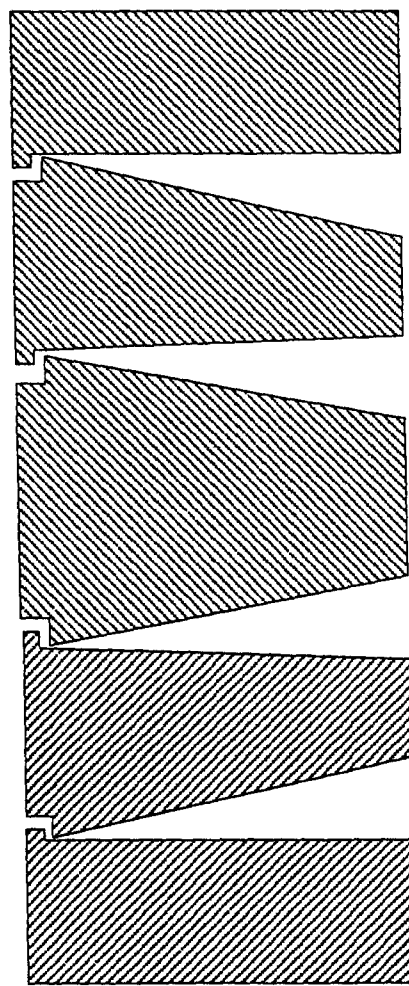


Fig. 8: Schematic drawing of the "non-recessed" nozzle.

In the Double Eagle experiments, the Ar K-shell x-ray yield using recessed nozzle is much high than that of non-recessed one. Using the AASC 4-channel Fiber Optic Interferometer (FOI), we have extensively characterized the gas puff flow produced from the "recessed" nozzle. The gas flow at three axial locations was scanned by FOI, providing a complete space and time map of the gas density. Fig. 9 shows one of the samples of the gas profile measured by FOI as a function of radius and time at $z=5$ mm downstream of the nozzle. The nozzle plenum pressures

for the inner and outer argon gas shells were the same, 24.7 psia. A rise time of $\approx 140 \mu\text{s}$ is observed.

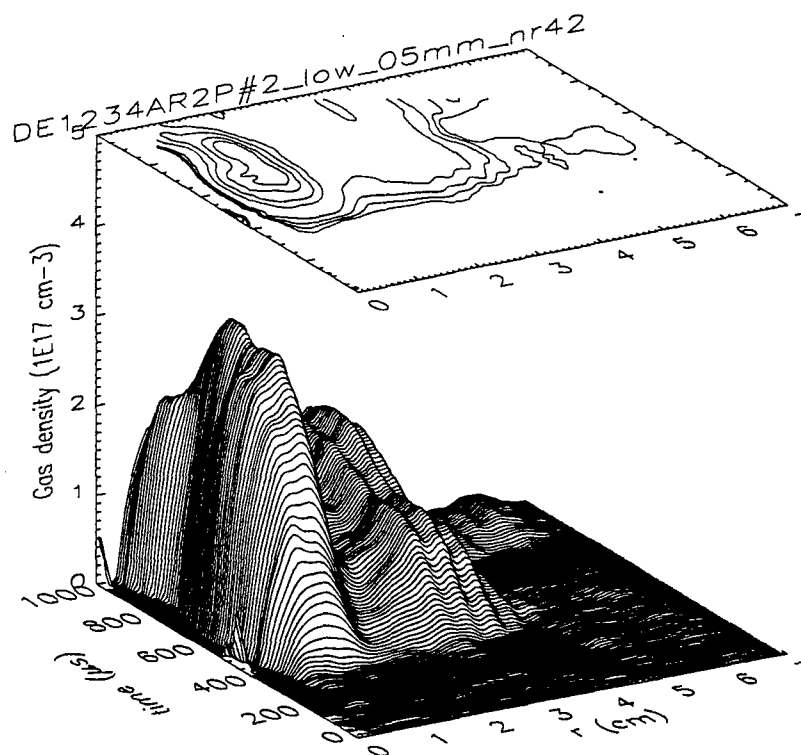


Fig. 9: FOI measured density as a function of time and radius at $z=0.5$ cm downstream. Titan-style recessed aerodynamic nozzle was used to produce the gas jet.

The “recessed” nozzle produces gas jets, which are merged to each other. The gas density gradient is small compared to that produced by the “non-recessed” nozzle. Since the LWA measures the gradient of the density-length product, signal/noise ratio is very poor in the case of the recessed nozzle even at 100 psia nozzle plenum pressures. Therefore, for this first evaluation of the LWA as a gas profile probe, a non-recessed nozzle was used with the pressure in the nozzle plenums set at 100 psia to increase the signal/noise ratio. Fig. 10 shows the LWA measured gas density profile at $t=400 \mu\text{s}$ after gas started to flow. The nozzle plenum pressures for the inner and outer argon gas shells were same. Shell structures of the gas puff are clearly visible. However, beyond 1 cm from the nozzle, the signal/noise starts getting poor. As shown in Fig. 10, the density-length product due to the gas puff is about 10^{18} cm^{-2} . Recalling that the air density-length product along the laser path was on the order of 10^{21} cm^{-2} , 0.1% perturbations in the laser air path could make large uncertainties. In the case of the LWA measurements, the pressure in the nozzle plenum was about 4 times high than that in the FOI measurement. Thus, a factor of ~ 4 times of the peak density between the two measurements is expected. But, our measurements suggest that the peak pressure difference is only about a factor 2. This could be

caused by not full opening of the gas valve at ~ 100 psia pressures. The agreement between the two techniques is fair. Clearly, the noise level of the LWA needs to be reduced to achieve higher quality results.

Further improvements of the LWA sensitivity can be made by placing the system in vacuum to reduce the air density-length product along the laser path by a factor of 100 or higher.

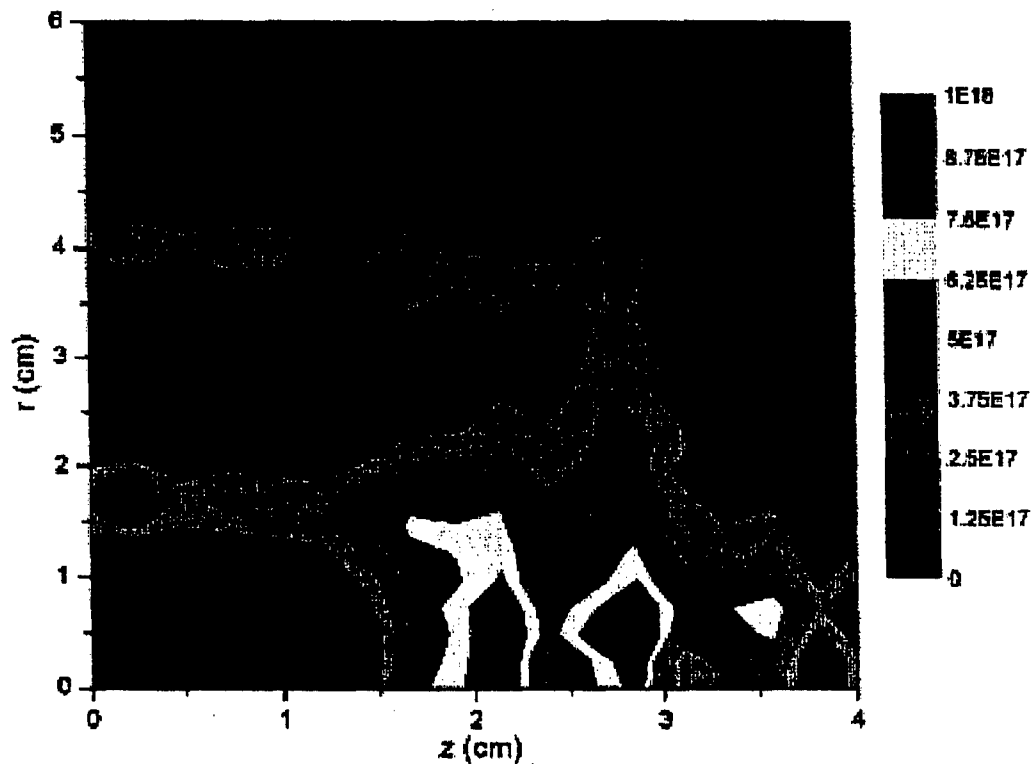


Fig. 10: Measured gas density (atoms cm^{-3}) profile at $t=400 \mu\text{s}$ after the starting of the gas puff flow by using LWA.

3. Summary and conclusions

We have developed a LWA suitable for gas puff density profile measurements. The advantage of the LWA is that the gas density profile can be obtained within one or few shots. However, in the present LWA configuration, the air density-length product ($\sim 10^{21} \text{ cm}^{-2}$) along the line of sight is much higher than that of gas puff ($\sim 10^{18} \text{ cm}^{-2}$). Variations in the air column limit

the present setup to a sensitivity of $\frac{d}{dx} \int n(\text{cm}^{-3}) dl(\text{cm}) \approx 5 \times 10^{17} \text{cm}^{-3}$. We have observed in FOI measurements that the time scale of the air turbulence is on the order of 1 ms. The effects of the air turbulence can be minimized to a factor of ≈ 10 when the reference image is taken within $\approx 500 \mu\text{s}$ of the gas measurement image by using two laser probe beams and/or by putting the LWA in a vacuum to reduce the air density-length product. With these improvements, the position uncertainty of the microlens focal spots can be reduced from the present 0.1 pixel to 0.01 pixels. Using a 3 fold increase (to 10:1) image demagnification system, the LWA sensitivity, $\frac{d}{dx} \int n(\text{cm}^{-3}) dl(\text{cm})$, could be improved to $\approx 10^{16} \text{cm}^{-3}$, which is close to the requirement for a reasonable characterization of the DQ gas puff hardware.

References

1. I. Ghozeil, "Hartmann and other screen tests," in Optical Shop Testing, edited by D. Malacara, John Wiley & Sons, New York, (1992), p.367.
2. J. L. Rayces, "Exact relation between wave aberration and ray aberration," Opt. Acta 11, 85 (1964).

**DISTRIBUTION LIST
DTRA-TR-03-17**

DEPARTMENT OF DEFENSE

DEFENSE TECHNICAL
INFORMATION CENTER
8725 JOHN J. KINGMAN ROAD,
SUITE 0944
FT. BELVOIR, VA 22060-6201
2 CYS ATTN: DTIC/OCA

DEFENSE THREAT REDUCTION
AGENCY
8725 JOHN J. KINGMAN ROAD,
STOP 6201
FT. BELVOIR, VA 22060-6201
2 CYS ATTN: NTES/R. DAVIS

**DEPARTMENT OF DEFENSE
CONTRACTORS**

ITT INDUSTRIES
ITT SYSTEMS CORPORATION
1680 TEXAS STREET, SE
KIRTLAND AFB, NM 87117-5669
2 CYS ATTN: DTRIAC
ATTN: DARE

ALAMEDA APPLIED SCIENCES
CORPORATION
626 WHITNEY STREET
SAN LEANDRO, CA 94577-0599
ATTN: M. KRISHNAN